Methylresorcinarene: A Reaction Vessel to Control the Coordination Geometry of Copper(II) in Pyridine *N*-oxide Copper(II) Complexes

Ngong Kodiah Beyeh, and Rakesh Puttreddy*

Department of Chemistry, Nanoscience Center, P. O. Box 35, 40014 University of Jyvaskyla, Finland

Supporting Information

Table of Contents

I General Information

All the solvents used for syntheses and crystal growth are reagent grade, and are used as received. Pyridine *N*-oxide **2**, 2-picolinic acid N-oxide **3** and $CuCl_2$ were purchased from Sigma Aldrich while $Cu(NO_3)_2.3H_2O$ from Merck & Co. Methylresorcinarene **1** was synthesized according to reported procedures.[1] The ^1H NMR spectra were recorded on a Bruker Advance DRX 500 MHz and DRX 400MHz spectrometers and solvents used for ^1H NMR analysis are purchased from Sigma Aldrich.

II Syntheses of complexes

Synthesis of complex I

To a solution of host **1** (20 mg, 0.0304 mmol) in methanol (5 ml) was added a methanol (2 ml) solution of pyridine *N*-oxide, **3** (3.0 mg, 0.0304 mmol) at room temperature. The solution was left at room temperature and subjected to slow evaporation to give brown colour crystals. Yield: 65%. Elemental Analysis: Calculated for $C_{40}H_{48}O_8.C_5H_5NO.3H_2O$: C 67.06; H 7.38; N 1.74. Found for $C_{40}H_{48}O_8.C_5H_5NO.3H_2O$: C 67.51; H 6.88; N 1.21. ^1H NMR (500 MHz, CD_3OD, 303 K) δ: 8.10 (d, 2H, J 5.85 Hz, NPh-H), 7.10 (s, 4H, Ar-H), 7.09 (t, 2H, J 6.95 Hz, NPh-H), 7.01 (t, 2H, J 7.62 Hz, NPh-H), 4.24 (t, J 7.87 Hz, 4H, CH), 2.21 (m, 8H, CH_2), 2.00 (s, 12H, Ar-CH_3), 0.91 (t, J 7.17 Hz ,12H, CH_3); ^{13}C NMR (100 MHz, 300 K, CD_3OD) δ: 149.5, 138.6, 129.5, 126.5, 124.9, 120.0, 112.1, 36.5, 26.7, 11.7, 8.3.

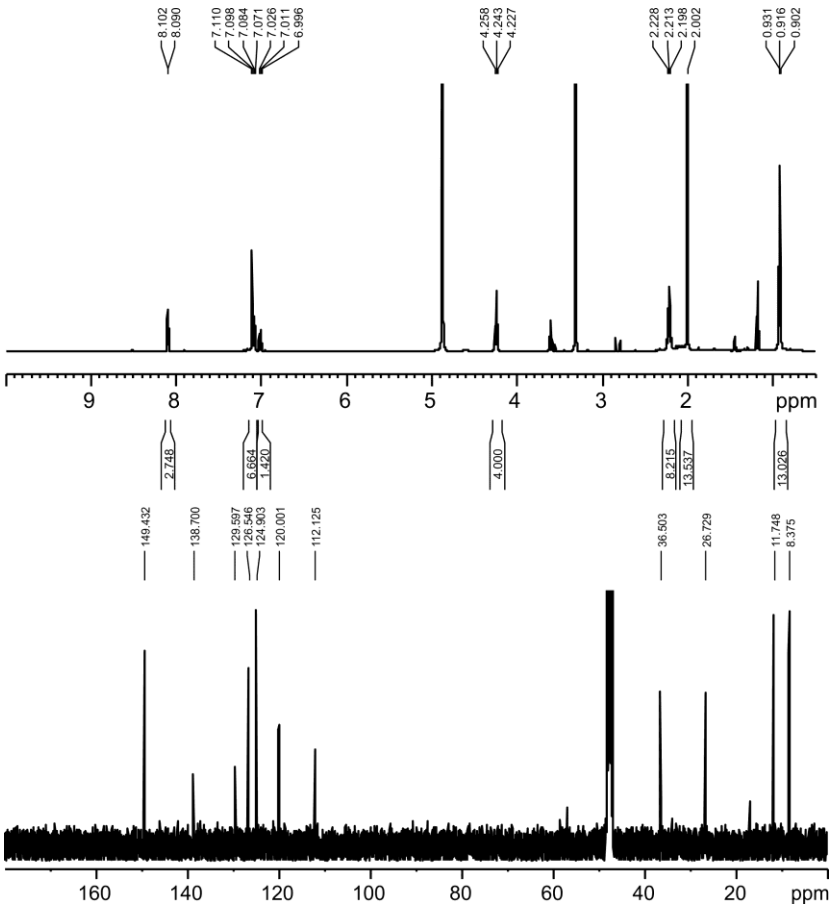

Figure S1. ^{1}H and ^{13}C NMR of assembly **I**.

Synthesis of complex II

To a solution of host **1** (20 mg, 0.0304 mmol) in methanol (5 ml) was added a methanol (2 ml) solution of 2-picolinic acid *N*-oxide, **3** (4.0 mg, 0.0304 mmol) at room temperature. The solution was left at room temperature and subjected to slow evaporation to give brown colour crystals. Yield: 49%. Elemental Analysis: Calculated for $C_{40}H_{48}O_8.C_6H_5NO_3.3H_2O$: C 65.00; H 7.00; N 1.65. Found: C 64.66; H 6.53; N 1.29. ^{1}H NMR (500 MHz, CD_3OD, 303 K) δ: 7.87 (d, 1H, J 7.90 Hz, NPh-H), 6.35 (d, 1H, J 5.85 Hz, NPh-H), 7.12 (s, 4H, Ar-H), 6.78 (t, 1H, J 7.75 Hz, NPh-H), 6.59 (t, 2H, J 6.17 Hz, NPh-H), 4.24 (t, J 7.87 Hz, 4H, CH), 2.21 (m, 8H, CH_2), 1.98 (s, 12H, Ar-CH_3), 0.91 (t, J 7.17 Hz,12H, CH_3); ^{13}C NMR (100 MHz, 303 K, CD_3OD) δ: 149.5, 137.9, 131.8, 129.0, 128.0, 124.9, 119.9, 112.1, 36.4, 26.6, 11.7, 8.3.

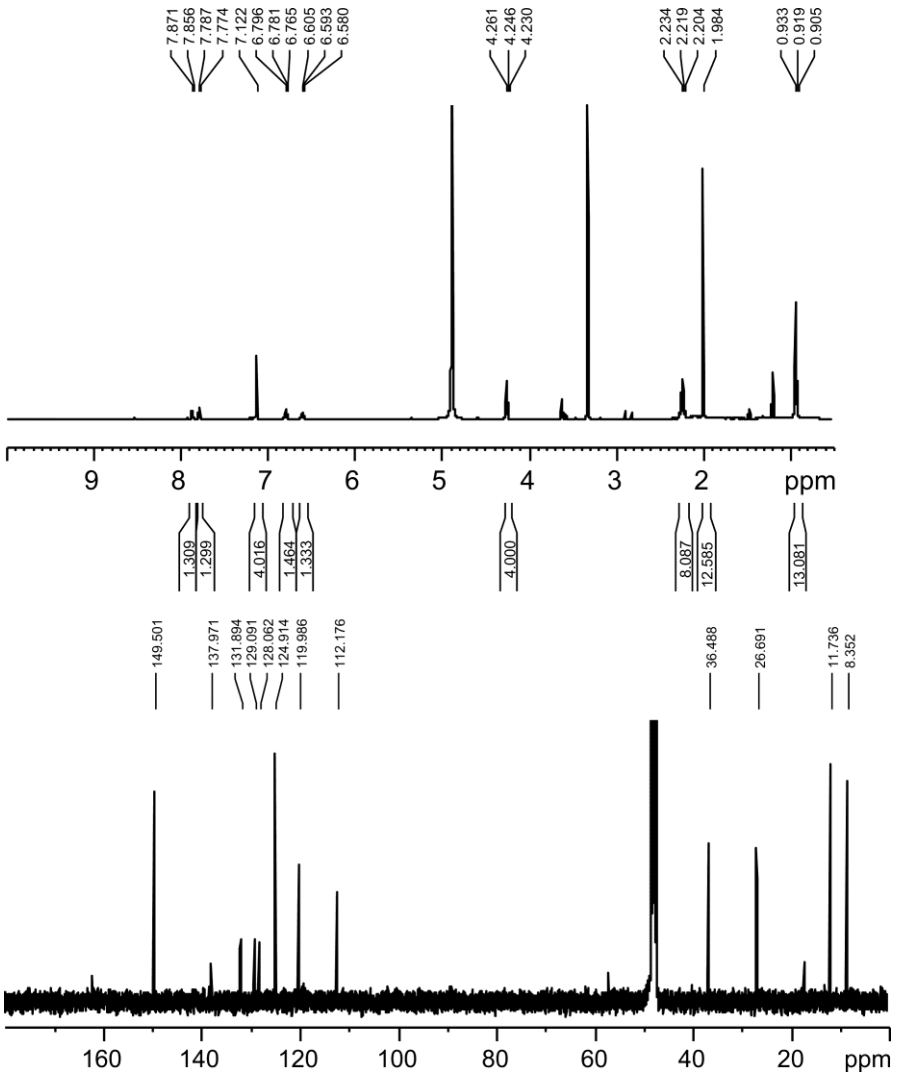

Figure S1. ^{1}H and ^{13}C NMR of assembly **II**.

Synthesis of complex III

To a solution of pyridine *N*-oxide, **3** (10 mg, 0.1051 mmol) in methanol (2 ml) was added a methanol (5 ml) solution of $CuCl_2$ (14 mg, 0.1051 mmol) at room temperature. The solution was left at room temperature and subjected to slow evaporation to give brown colour crystals. Yield: 87.6%. Elemental Analysis: calculated for $C_5H_5NO.CuCl_2$: C 26.16; H 2.20; N 6.10. Found: C 26.55; H 1.89; N 5.92.

Synthesis of complex V

To a solution of 2-picolinic acid *N*-oxide (10 mg, 0.0718 mmol) in methanol (2 ml) was added a methanol (2 ml) solution of $Cu(NO_3)\cdot 3H_2O$ (17 mg, 0.0718 mmol) at room temperature. The solution was left at room temperature and subjected to slow evaporation to

give brown colour crystals. Yield: 94%. Elemental Analysis: calculated for [2($C_6H_5NO_3$).Cu]: C 42.42; H 2.37; N 8.25. Found: C 42.61; H 2.91; N 8.02.

Syntheses of complexes IV and **VI**

In a typical reaction for complexes **IV** and **VI**, 1:1:1 molar ratio of host **1,** guest and Cu^{II} salts of individual methanol solutions are mixed and left at room temperature for slow evaporation. The resultant solution yields brown colour crystals suitable for X-ray analysis. The obtained crystals were measured immediately, and are highly unstable to carry out detailed characterization.

III X-ray Analyses

a) X-ray experimental

Single crystal X-ray data for **I, III** and **IV** were collected at 170 K using a Bruker-Nonius Kappa CCD diffractometer with an APEX-II detector and graphite monochromatized Mo-Kα (λ = 0.71073 Å) radiation; the data for **VI** was measured at 170 K with Agilent SuperNova single-source diffractometer equipped with an Atlas EoS CCD detector using mirror-monochromated Mo-*K*α (λ = 0.71073 Å) radiation, while data collections for **II** and **V** (Fig. S4a) were performed at 123 K with Agilent Super-Nova dual source wavelength diffractometer with an Atlas CCD detector using multilayer optics monochromatized Cu- Kα (λ = 1.54184 Å) radiation. The data collection and reduction for **I, III** and **IV** were performed using the program *COLLECT*[2] and *HKL DENZO AND SCALEPACK*[3], respectively. The data collection and reduction for **II, V** and **VI** were performed using the program *CrysAlisPro*[4]. For **I**, **III** and **VI**, the intensities were corrected for absorption using *SADABS*[5] with multi-scan absorption correction type method. Gaussian face index absorption correction method[4] was used for **II**, **V** and **VI**. All the structures were solved with direct methods (*SHELXS*[6]) and refined by full-matrix least squares on F^2 using the *OLEX2*[7], which utilizes the *SHELXL*-2013 module[6]. No attempt was made to locate the hydrogens for some solvent molecules, and for some hydrogen atoms involved in hydrogen bonds were introduced from difference Fourier maps. Constraints (EADP) and restraints (DFIX and ISOR) are used where appropriate, and for disordered solvent molecules.

b) Solid state discussion

The host-guest interactions between the electron rich host **1** and electron deficient N-oxide guest molecules have caused significant changes in the conformation of host **1**. These conformational changes in host **1** play a crucial role in determining the coordination environment around copper(II). As shown in Fig. S2, the centroid-to-centroid distances are calculated between the mean-planes of the opposite aromatic rings in the host **1**, and are used to highlight the breathing properties. Though Fig. S2a, S2d and S2b, S2c are obtained from different composites, they have adopted near similar centroid-to-centroid distances. This fact explains the reason for the change in coordination environment around copper(II) by *cis-trans*

transformation between **III** and **IV,** and O6 to O4 coordination geometry between **V** and **VI**. The absence of metal coordination results in expansion in Fig. S2a and contraction in Fig. S2b, which imposes a "slightly tilted" behaviour for pyridine N-oxide (Fig. 4a) and "standing" behaviour for planar (aromatization followed by intramolecular) 2-picolinic acid N-oxide (Fig. 4b) offering π-π interaction.

In Fig. S2c, the host inhales exhibiting steric hindrance preventing pyridine N-oxide from bidentate coordination mode to form L_2M_2 complex. On the other hand, in Fig. S2d, host exhales accommodating water molecules to approach apically square planar copper(II) by exhibiting weak interactions (see also Fig. S4b).

Table S1. Crystallographic details for structures of **I-III**

Complex	**I**	**II**	**III**
Empirical formula	$C_{45}H_{59}NO_{12}$	$C_{46}H_{53}NO_{14}$	$C_5H_5Cl_2NOCu$
Formula weight	805.93	843.89	229.54
Temperature (K)	170.0	123.0	170.0
Crystal system	Triclinic	Triclinic	Monoclinic
Space group	*P*-1	*P*-1	$P2_1/c$
Unit cell dimensions: a (Å)	12.163(2)	11.4574(6)	5.8340(12)
b (Å)	12.581(3)	11.5478(6)	13.603(3)
c (Å)	15.876(3)	17.0220(8)	9.863(2)
α (°)	71.47(3)	77.408(4)	90
β (°)	73.69(3)	87.270(4)	105.34(3)
γ (°)	69.55(3)	74.490(5)	90
Volume / $Å^3$	2118.4(10)	2117.8(2)	754.8(3)
Z	2	2	4
Density (calculated) mg/m^3	1.263	1.323	2.020
Absorption Coefficient mm^{-1}	0.091	0.812	3.523
F(000)	864	896	452
Crystal size (mm^3)	0.27 x 0.25 x 0.19	0.25 x 0.15 x 0.12	0.41 x 0.38 x 0.37
θ range for data collection (°)	2.1 to 25.3	4.0 to 66.7	2.6 to 25.3
Reflections collected [R(int)]	19133 [0.0622]	13282 [0.0284]	6631 [0.0635]
Observed reflections [I>2σ(I)]	4264	5956	1099
Data completeness (%)	98.90	99.10	99.99
Data/ restraints/ parameters	75710/540	7430/1/635	1361/0/91
Goodness-of-fit on F^2	1.101	1.059	1.051
Final R_1 indices [I>2σ(I)]	$R_1 = 0.0980$, $wR_2 = 0.2383$	$R_1 = 0.0520$, $wR_2 = 0.1420$	$R_1 = 0.0381$, $wR_2 = 0.0707$
Final R indices [all data]	$R_1 = 0.1700$, $wR_2 = 0.2734$	$R_1 = 0.0642$, $wR_2 = 0.1558$	$R_1 = 0.0579$, $wR_2 = -0.711$
Largest diff. peak/hole ($e.Å^{-3}$)	0.373/ -0.344	0.731/ -0.428	0.621/ -1.069

Table S2. Crystallographic details for structures of **IV-VI**

Complex	**IV**	**V**	**VI**
Empirical formula	$C_{94}H_{120}Cl_2N_2O_{28}Cu$	$C_{12}H_8N_2O_6Cu$	$C_{92}H_{112}N_2O_{28}Cu$
Formula weight	1860.35	339.74	1757.37
Temperature (K)	170.0	123.0	170.0
Crystal system	Triclinic	Monoclinic	Triclinic
Space group	*P*-1	$P2_1/c$	*P*-1
Unit cell dimensions: a (Å)	12.163(2)	3.6410(6)	12.1909(7)
b (Å)	12.630(3)	12.6301(17)	12.7422(6)
c (Å)	16.953(3)	12.1194(13)	15.5226(9)
α (°)	105.26(3)	90	81.845(4)
β (°)	101.94(3)	94.057(13)	73.601(5)
γ (°)	97.56(3)	90	69.069(5)
Volume / $Å^3$	2410.0(9)	555.93(14)	2158.3(2)
Z	1	2	1
Density (calculated) mg/m^3	1.282	2.030	1.352
Absorption Coefficient mm^{-1}	0.359	3.139	0.336
F(000)	985	342	931
Crystal size (mm^3)	0.24 x 0.17 x 0.11	0.12 x 0.03 x 0.03	0.15 x 0.14 x 0.09
θ range for data collection (°)	1.8 to 25.3	5.1 to 66.7	3.1 to 25.3
Reflections collected [R(int)]	24687 [0.0719]	1617 [0.0834]	14471 [0.0393]
Observed reflections [I>2σ(I)]	5313	700	5613
Data completeness (%)	99.80	98.67	99.83
Data/ restraints/ parameters	8722/48/649	975/0/97	7807/12/615
Goodness-of-fit on F^2	1.022	1.077	1.093
Final R_1 indices [I>2σ(I)]	$R_1 = 0.0785$, $wR_2 = 0.1681$	$R_1 = 0.0826$, $wR_2 = 0.2050$	$R_1 = 0.0755$, $wR_2 = 0.2005$
Final R indices [all data]	$R_1 = 0.1389$, $wR_2 = 0.1973$	$R_1 = 0.1056$, $wR_2 = 0.2401$	$R_1 = 0.1070$, $wR_2 = 0.2229$
Largest diff. peak/hole ($e.Å^{-3}$)	0.528/ -0.673	1.380/ -1.069	0.839/ -1.117

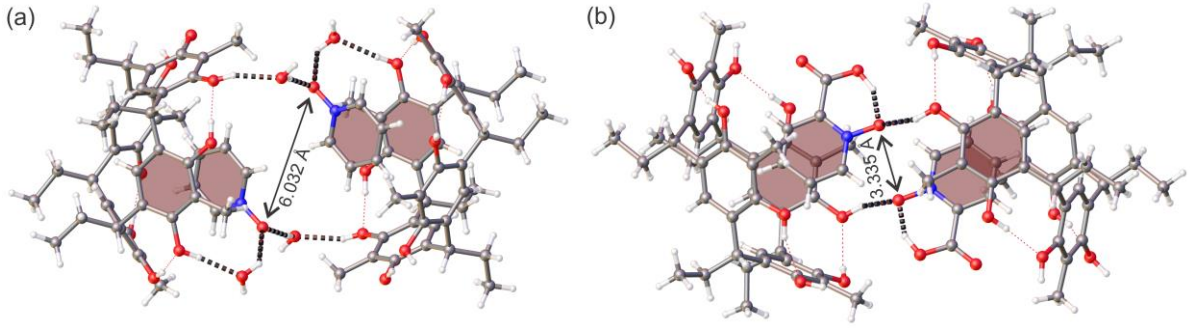

Fig. S3. Two hydrogen bonded 1:1 host-guest complexes of (a) complex **I**, and (**b**) complex **II**. Hydrogen bonds are shown in black broken lines, and the distances between oxygens of N-O groups inside the host of guest molecules **2**, **3** are shown with solid double headed arrow.

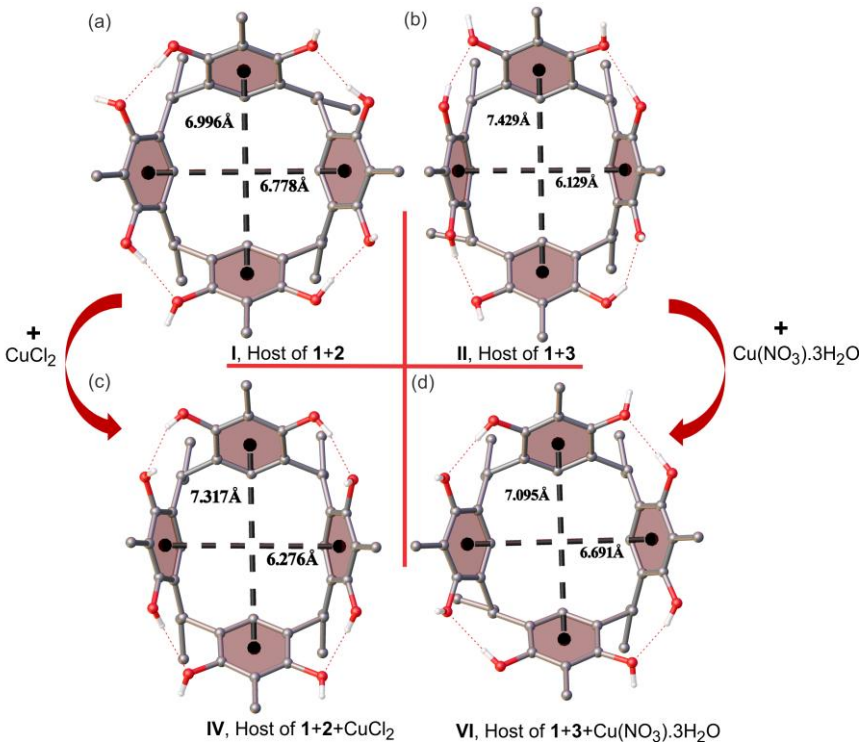

Fig. S4. Breathing properties of host **1**. Selected hydrogen atoms, guest and solvent molecules are omitted for clarity.

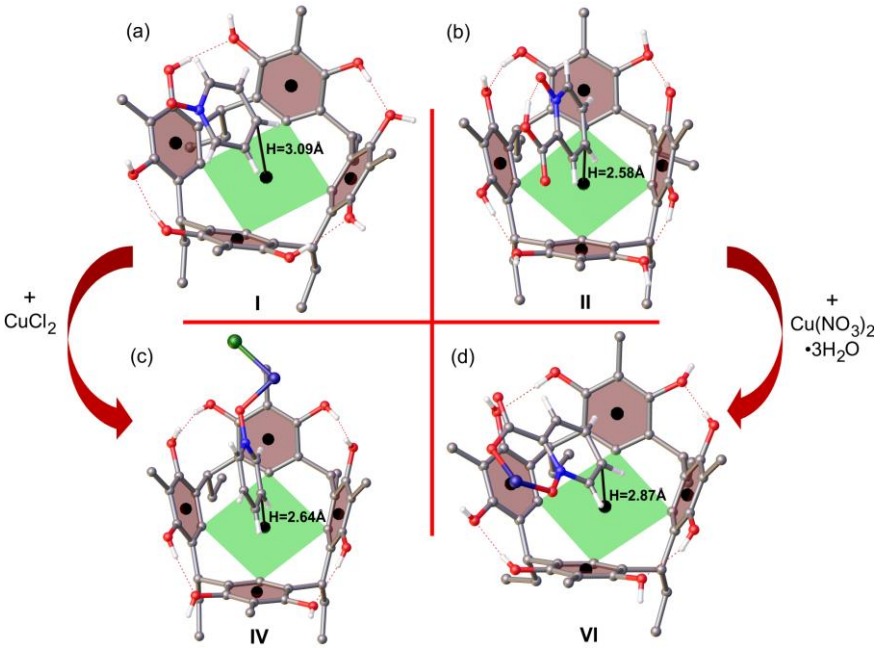

Fig. S5. Accommodation of guest molecules and height (distances are calculated from centroid-to-centroid of bottom ring carbon atoms) calculations. Selected hydrogen atoms, guest and solvent molecules are omitted for clarity.

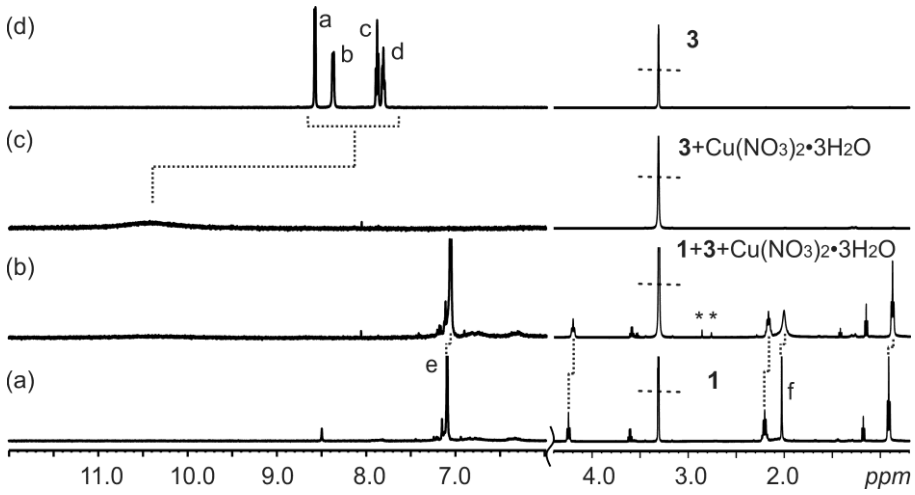

Fig. S6. ^{1}H NMR spectra (CD_3OD, 303 K) of a 30 mM solution of (a) **1**, (b) equimolar mixture of **1**, **3** and $Cu(NO_3)_2{\cdot}3H_2O$, (c) equimolar mixture of **3** and $Cu(NO_3)_2{\cdot}3H_2O$, (d) **3**. The shift changes are highlighted by the dotted lines. Stars represent water molecules present in the complex (see Fig 5).

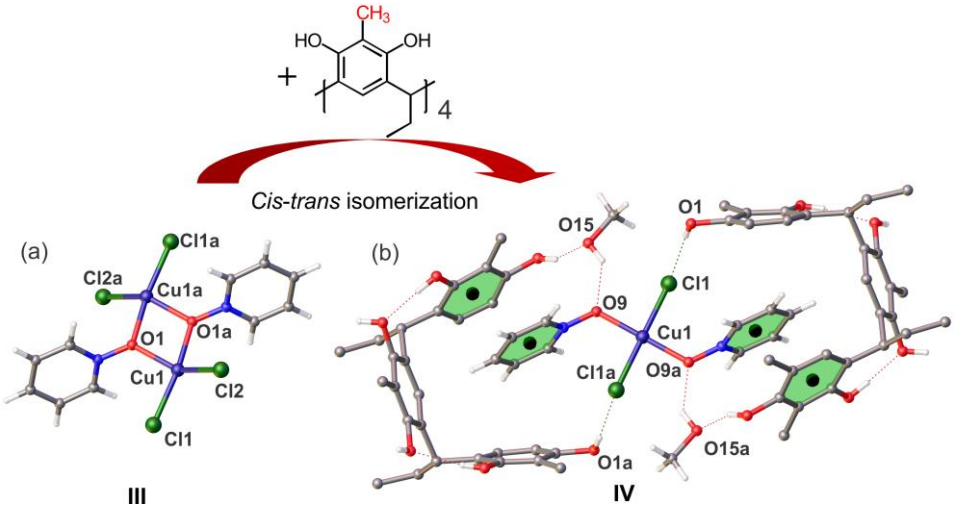

Fig. S7. *Cis-trans* isomerization with host **1.** Change in denticity of guest due to steric hindrance created by host and guest π-π interaction.

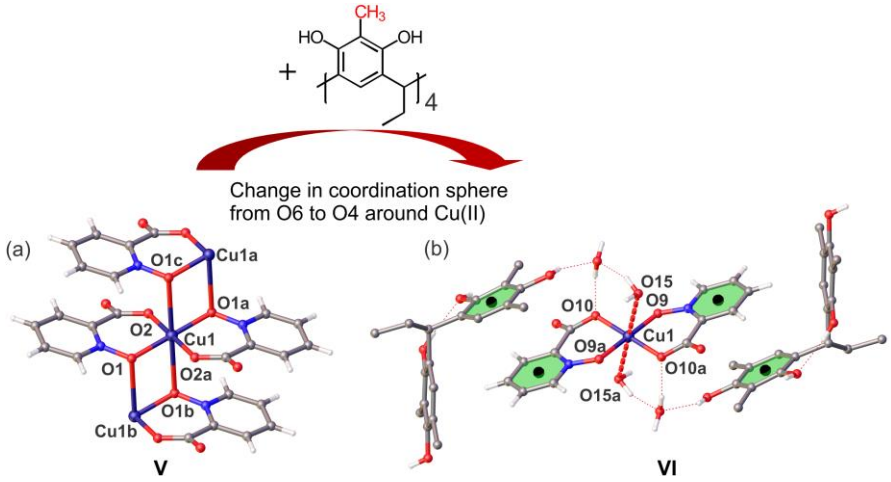

Fig. S8. Change in coordination number around Cu(II) due to steric hindrance engendered by host **1**.

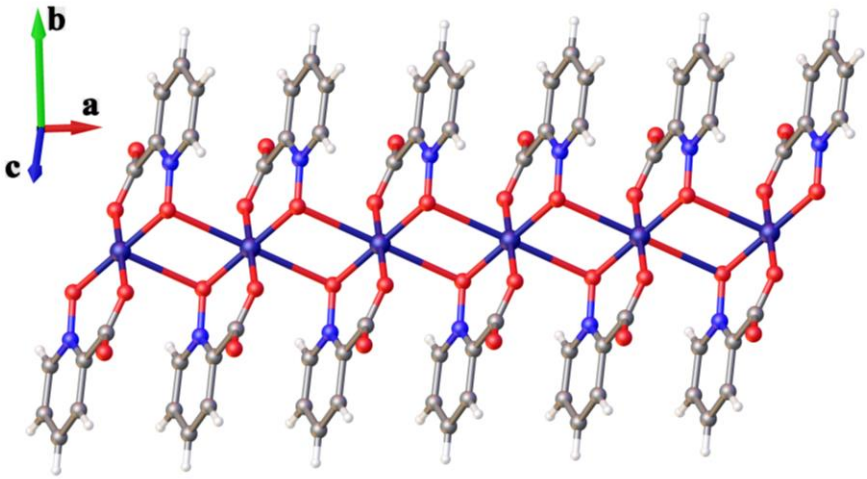

Fig. S9. 1-D Polymeric structure of complex **V**.

III References

1. a) P. Timmerman, W. Verboom and D. Reinhoudt, *Tetrahedron,* 1996, **52**, 2663–2704; b) A. Jasat and J. C. Sherman, *Chem. Rev.,* 1999, **99**, 931–967.
2. Bruker AXS BV, Madison, WI, USA; 1997–2004.
3. Z. Otwinowski and W. Minor, *Methods Enzymol.,* 1997, **276**, 307–326.
4. *CrysAlisPro* 2012, Agilent Technologies. Version 1.171.36.35.
5. R. H. Blessing, *J. Appl. Cryst.,* 1997, **30**, 421–426.
6. G. M. Sheldrick, *Acta Cryst. A* 2008, **64**, 112–122.
7. O. V. Dolomanov, L. J. Bourhis, R. J. Gildea, J. A. K. Howard and H. Puschmann, *J. Appl. Cryst.* 2009, **42**, 339–341.